

Study of base doping rate effect on parallel vertical junction silicon solar cell under magnetic field

¹ Mohamed Iemine OULD CHEIKH
, ² Boureima SEIBOU, ¹ Mohamed Abderrahim Ould El Moujtaba , ¹ Khady FAYE,
³ Mamadou WADE, ¹ Grégoire SISSOKO

- (1) Laboratory of Semiconductors and Solar Energy, Physics Department, Faculty of Science and Technology, University Cheikh Anta Diop, Dakar, Senegal
(2) Mines, Industry and Geology School of Niamey- Niger
(3) Electromechanical Engineering Department, Polytechnic School of Thies – Sénégal

Abstract:

In this work we suggest looking for influences of a constant magnetic field and the base doping rate on a parallel vertical junction silicon solar cell under multispectral illumination in static regime. A study on the coefficient and the length diffusion according to the magnetic field B and the doping rate N_b is made. The minority carriers density in the base was studied according to the depth of the base for various values of the base doping rate and the magnetic field. This study allows us to determine the influences of the doping rate and the magnetic field on the photocurrent density, the photovoltage, the space charge region capacitance. The study of these electrical parameters is done according to the concept of the junction surface recombination velocity of excess minority carriers. The logarithm of the capacitance versus photovoltage leads to transitional capacitance.

Keywords: Parallel vertical junction solar cell – Magnetic field – Doping rate

1 Introduction

The improvement of the performances and the quality of solar cells is one concern major to which the current research turns. Thus, the basic material for manufacturing solar cells benefit ceaselessly technological progress as well on the mode of the manufacturing and the increase substrates as on the final structure of the solar cell elaborated. For that purpose, many research are done on conventional solar cells, solar cells with back field or B.S.F (Back Surface Field) [1,2],

monocrystalline and polycrystalline monofacial silicon solar cells, polycrystalline and monocrystalline bifacial silicon solar cell [3], vertical junctions solar cells, solar cells with concentration...

The purpose of this article is to do a study on a parallel vertical junction silicon solar cell under multispectral illumination in static regime. A theoretical study of the excess minority carriers in the base of the solar cell is produced through continuity equation. With help of the boundary conditions at the junction and at the middle of the base, excess minority carriers density are studied and lead to the expression of photocurrent density and photovoltage. From the well-known I-V characteristic of the solar cell under illumination, electrical equivalent model is established for low and high junction recombination values giving respectively ideal generator source of tension and current. Series and shunt resistances are then deduced.

Space charge region capacitance is expressed depending on junction recombination velocity. Logarithm of the capacitance according to the photovoltage gives the intrinsic capacitance.

2 Theoretical study

2.1 Solar cell description

A Parallel vertical junction silicon solar cell under constant multispectral illumination in static regime of

type $n^+ - p - n^+$ [4-5], is presented on figure 1. The illumination is carried out according to Oz axis. The magnetic field B is represented perpendicularly to the (xOz) plan.

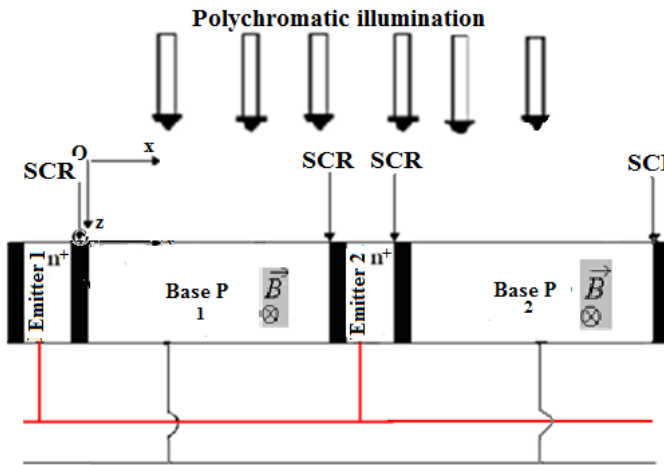


Figure 1: Schema of a parallel vertical junction solar cell under magnetic field

2.2 Continuity equation

The continuity equation relative to the excess charge carrier density in the base is expressed as follows:

$$\frac{\partial^2 \delta(x)}{\partial x^2} - \frac{\delta(x)}{L^*2} = -\frac{G(z)}{D^*} \tag{Eq - 1}$$

Where $\delta(x)$ is the excess minority carrier (i.e. electron), in the p-base of thickness H.

$G(z)$ is the carrier generation rate, its expression is given by the following relation [6]:

$$G(z) = \sum_{i=1}^3 a_i e^{-b_i z} \tag{Eq - 2}$$

Parameters a_i and b_i are coefficients deduced from solar radiation under AM 1,5.

$D^* = D(Nb, B)$ [7,10-13] represents the diffusion coefficient of electrons generated in the base, it depends on magnetic field and doping rate, its expression is :

$$D^*(B, Nb) = \frac{D}{[1 + (\mu B)^2] \sqrt{1 + \frac{81 \times Nb}{Nb + (3,2 \times 10^{18})}}} \tag{Eq - 3}$$

D is diffusion coefficient without magnetic field ($D=35\text{cm}^2.\text{s}^{-1}$), μ is the electron mobility. Profile of diffusion coefficient according to magnetic field B and the doping rate of the base Nb is given on the following figure:

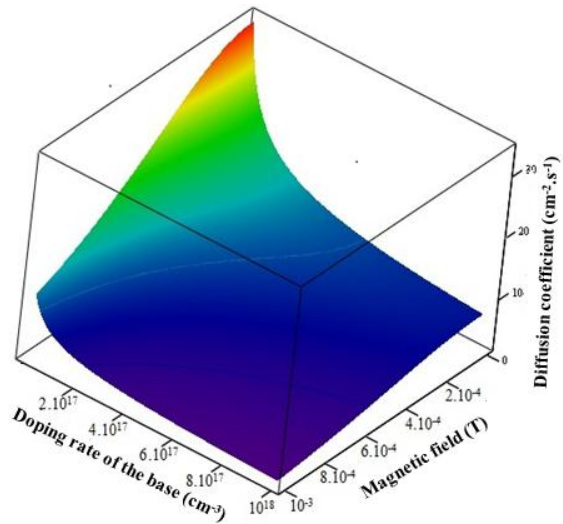


Figure 2: Profile of diffusion coefficient according to magnetic field B and the doping rate Nb of the base $\mu=1350\text{cm}^2.\text{V}.\text{s}^{-1}$, $D=35\text{cm}^2.\text{s}^{-1}$

For the low magnetic field values, the diffusion coefficient remains constant, but when the field values become more significant, the diffusion coefficient begins to decrease. It can be explained by the magnetic field effect which slows down or diverts the minority carriers. The curve above presents two regions: the first one $10^{-6} \text{ T} \leq B \leq 10^{-4} \text{ T}$, and the second for $B > 10^{-4} \text{ T}$. The low magnetic fields ($B \leq 10^{-4} \text{ T}$) are without effect on the minority carrier’s diffusion; however it is strongly affected for magnetic field values beyond 10^{-4} T . So we can see the strong reduction of the diffusion coefficient which passes $26 \text{ cm}^2.\text{s}^{-1}$ at approximately $8 \text{ cm}^2.\text{s}^{-1}$. The carrier’s diffusion becomes quasi-impossible when the solar cell is plunged into a strong magnetic field ($B > 10^{-3} \text{ T}$).

We can observe on this figure that the diffusion coefficient also decreases with the base doping; indeed, if the doping of the base increases, the recombination phenomena also increase.

As for the magnetic field influence on the conduction phenomenon in the solar cell, we can use the diffusion length of the minority carriers which is linked to the diffusion coefficient.

L^* is the diffusion length of excess minority carriers when solar cell is placed under magnetic field. It's given by the following relation:

$$L^* = \sqrt{\tau(Nb)D^*} \quad (\text{Eq - 4})$$

$\tau(Nb)$ is the minority carriers lifetime.

It is expressed as [14]:

$$\tau(Nb) = \frac{12}{1 + \frac{Nb}{5 \times 10^{16}}} \quad (\text{Eq - 5})$$

The diffusion length profile according to magnetic field B and the doping rate of the base Nb is presented on figure3:

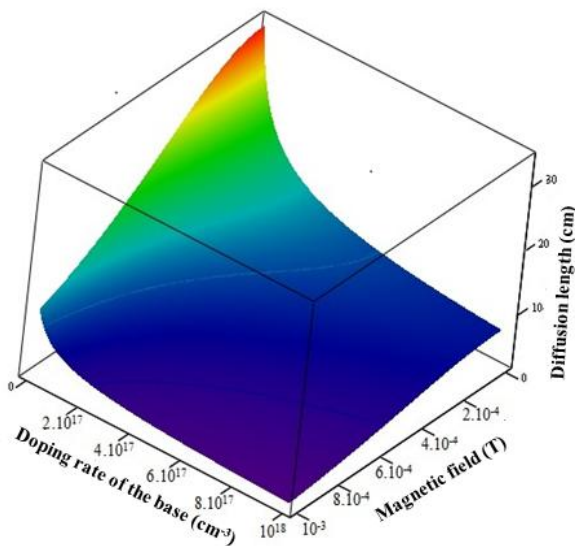


Figure 3 : Profile of diffusion length according to magnetic field B and the doping rate Nb of the base.

$$\mu = 1350 \text{ cm}^2 \cdot \text{V} \cdot \text{s}^{-1}, D = 35 \text{ cm}^2 \cdot \text{s}^{-1}$$

For the low magnetic field values, the diffusion length remains constant. But when the magnetic field becomes more and more important, the diffusion length decreases gradually. It can be explained by the magnetic field effect which slows down or diverts the minority carriers. We can observe also on this figure that the diffusion length decreases with the base doping rate.

The phenomena of diffusion, conduction and generation are linked by the continuity equation which has for general solution:

$$\delta(x, z, B, Sf, Nb) = A \cosh\left(\frac{x}{L^*}\right) + C \sinh\left(\frac{x}{L^*}\right) + \sum_{i=1}^3 K_i e^{-b_i z} \quad (\text{Eq - 6})$$

With

$$K_i = \frac{a_i L^{*2}}{D^*} \quad (\text{Eq - 7})$$

Where coefficients A and C are determined from the boundary conditions.

a) At Junction $x=0$:

$$\left. \frac{\partial \delta(x)}{\partial x} \right|_{x=0} = \frac{Sf}{D^*} \delta(x)|_{x=0} \quad (\text{Eq - 8})$$

Electrons undergo recombination at junction Emitter1-Base1 ($x = 0$) of the solar cell. This recombination at the junction is characterized by junction surface recombination velocity Sf [15-18].

At the middle of the base $x = H/2$:

$$\left. \frac{\partial \delta(x)}{\partial x} \right|_{x=H/2} = 0 \quad (\text{Eq - 9})$$

At the middle of the base, $x = H/2$, the gradient of the minority carriers density, far from the junction is null [19]. H is the solar cell the base thickness.

3 Results and discussion

3.1 Excess minority carriers density

We present on figure 4 the minority carriers density versus x , depth in the base for various applied magnetic field values:

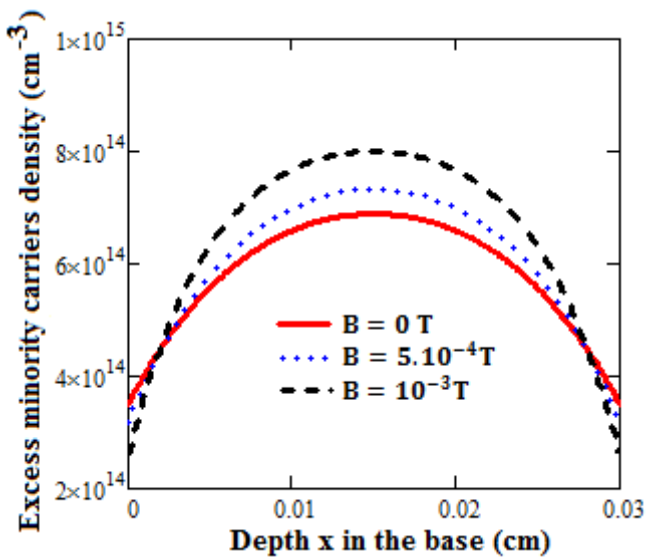


Figure 4 :Minority carriers Density in the base versus depth for various magnetic field

$N_b = 10^{17} \text{ cm}^{-3}$; $S_f = 3.10^3 \text{ cm} \cdot \text{s}^{-1}$; $D = 35 \text{ cm}^2 \cdot \text{s}^{-1}$
 $z = 0,0002 \text{ cm}$; $H = 0,03 \text{ cm}$

We note that in the zone $x < x_0$ ($x_0 = H/2$), the gradient of the minority carriers density is positive, and it corresponds to a passage of electrons flux giving a photocurrent in the junction emitter1-base1. For $x = x_0$, the minority carriers density in the base is maximal, its gradient is null. In region $x > x_0$, the gradient of the minority carriers density in the base is also positive because there is another junction between the base and the second emitter situated in the position $x = H$, we also note a passage of electrons flux in this junction.

Near the junctions, the minority carriers density decreases when the magnetic field intensity increases. More the electrons are photogenerated near to the junctions more they are likely of all to pass them (presence of junction surface recombination velocity), which gives us a minimal density at the various Base-emitter junctions. This phenomenon is accentuated in the presence of strong magnetic field. However near $x_0 = H/2$, the minority carriers density increases with the magnetic field. Indeed as we have already noted it, with

magnetic field presence, the charge carriers are deviated from their initial trajectory entailing a blocking in the base.

On figure 5 we give the profile of minority carriers density versus x , depth in the base for various doping rate values:

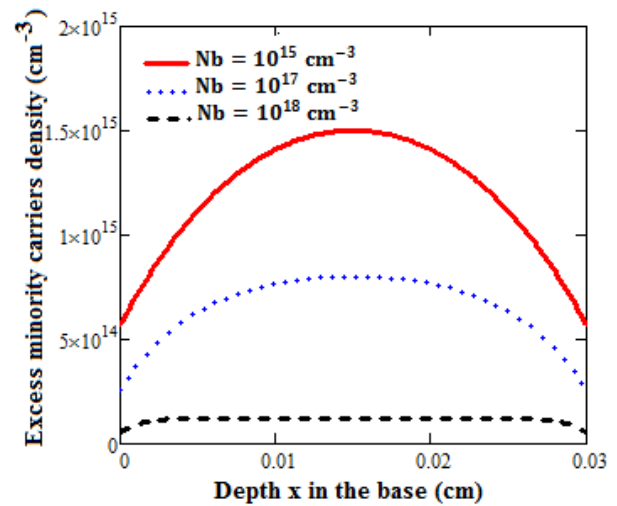


Figure 5:Minority carriers density in the base versus depth for various doping rate of the base N_b

$z = 0,0002 \text{ cm}$; $S_f = 3.10^3 \text{ cm} \cdot \text{s}^{-1}$ $B = 10^{-3} \text{ T}$;
 $D = 35 \text{ cm}^2 \cdot \text{s}^{-1}$; $H = 0,03 \text{ cm}$;

We observe that the minority carriers density decreases with doping rate of the base but this decrease is especially marked for the strong base doping. Indeed, if the base doping increases, it means that the impurities within the material increase: This entails an increase of recombination in bulk and consequently a decrease of the density of these carriers.

3.2 Photocurrent density:

The photocurrent density of a solar cell is deduced from the minority carriers density gradient at junctions. Its expression is given by:

$$J_{ph} = 2qD^* \left. \frac{\partial \delta(x, z, B, Nb)}{\partial x} \right|_{x=0} \quad (\text{Eq} - 10)$$

Where q is the elementary charge.

a) Magnetic field effect on photocurrent density :

Figure 6 illustrates the effect of magnetic field on the photocurrent density:

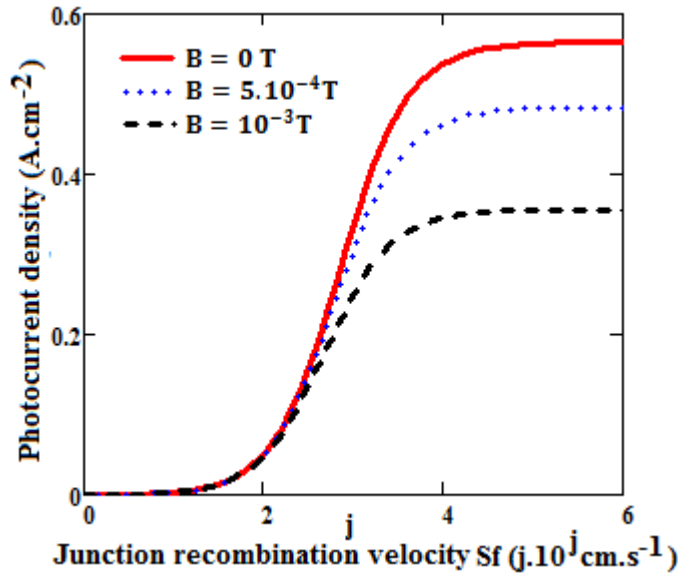


Figure 6 :Photocurrent density versus junction surface recombination velocity for various magnetic field.
 $z = 0,0002 \text{ cm}$; $D = 35 \text{ cm}^2 \cdot \text{s}^{-1}$; $N_b = 10^{17} \text{ cm}^{-3}$;
 $H = 0,03 \text{ cm}$

For a given magnetic field, the density of photocurrent increases with the junction surface recombination velocity S_f , which also indicates the operating point of the solar cell. Then we observe three regions.

- i) The first one for the low S_f values ($< 2.10^2 \text{ cm} \cdot \text{s}^{-1}$) corresponding to open circuit condition where the photocurrent density is minimal.
- ii) The second region, corresponds to high S_f values ($> 4.10^4 \text{ cm} \cdot \text{s}^{-1}$) and leads to short-circuit condition where photocurrent density is maximal (short circuit current).
- iii) The third region is located between, both first and second regions and represents current for operating points ($2.10^2 \text{ cm} \cdot \text{s}^{-1} < S_f < 4.10^4 \text{ cm} \cdot \text{s}^{-1}$), between open circuit and short circuit conditions (The photocurrent decreases with the magnetic field intensity, the low

magnetic field values are almost without effects on the photocurrent.

This decrease is due to the low flow minority carriers which cross the junctions base-emitter for contributing to photocurrent.

Doping rate effect on photocurrent density

Figure 7 illustrates variation of photocurrent density versus junction recombination velocity for various doping rate:

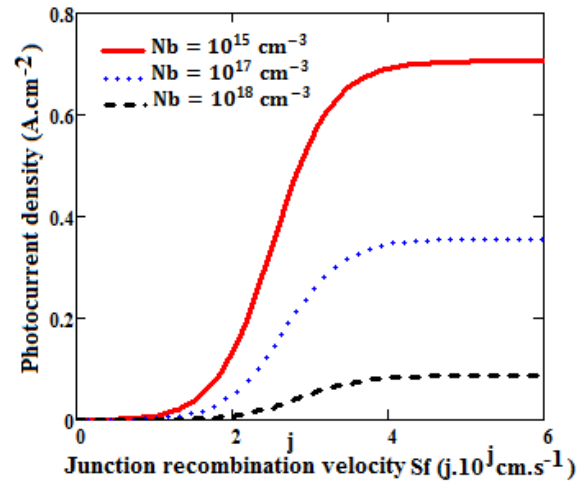


Figure 7:Photocurrent density versus junction recombination velocity for various doping rate of the base.
 $z = 0,0002 \text{ cm}$; $D = 35 \text{ cm}^2 \cdot \text{s}^{-1}$; $B = 10^{-3} \text{ T}$;
 $H = 0,03 \text{ cm}$

Figure 7 shows that the photocurrent density decreases with the doping rate of the base. These results are in good agreement with those found for diffusion coefficient of the minority carriers in the base. Indeed the carriers which cross the junction become low for strong doping rate. The increase of the doping rate induces an increase of impurities in the solar cell thus a large part of the minority carriers recombines in the base; that explains the diminution of the photocurrent with the doping rate.

3.3 Photovoltage

The photovoltage of the solar cell is determined by the Boltzmann’s expression :

$$V_{ph} = V_T \ln \left[1 + \frac{N_b}{N_0} \delta(x = 0, z) \right] \quad (\text{Eq - 11})$$

with $V_T = \frac{KT}{q}$ (Eq - 12)

Where N_0 is the intrinsic concentration of the minority carriers ($6,78.10^9 \text{ cm}^{-3}$) and N_b is the base doping rate (cm^{-3}). V_T is the thermal voltage and k is the Boltzmann’s constant ($1,38.10^{-23} \text{ m}^2 \text{ kg s}^{-2} \text{ K}^{-1}$). T is the absolute temperature.

a) Magnetic field effect on photovoltage :

On figure 8 is presented the profile of photovoltage versus junction surface recombination velocity for various magnetic field values:

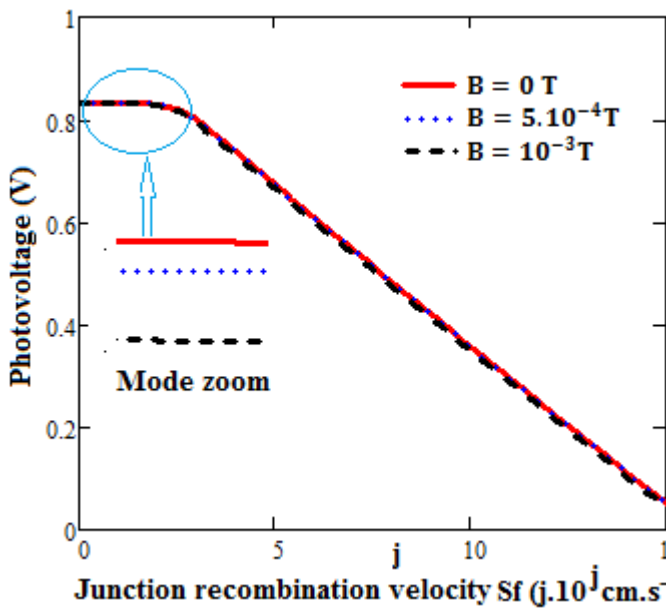


Figure 8: Photovoltage versus junction surface recombination velocity for various magnetic field values $z = 0,0002 \text{ cm}$; $D = 35 \text{ cm}^2. \text{s}^{-1}$; $N_b = 10^{17} \text{ cm}^{-3}$; $H = 0,03 \text{ cm}$

For a given magnetic field, the photovoltage decreases with junction recombination velocity. Indeed for low S_f values, the photovoltage is almost constant and

corresponds to the open circuit condition where excess minority carriers are blocked and stored at the junction. When the junction recombination velocity S_f increases, these charge carriers cross through the junctions, and then the photovoltage decreases.

Photovoltage also decreases when the magnetic field intensity increases. But this decrease is low near the open circuit. This decrease is explained by the fact that when the magnetic field increases, the minority carriers density near the junctions decreases.

b) Doping rate effect on photovoltage:

Profile of the photovoltage versus junction recombination velocity for different doping rate N_b is presented in the following figure.

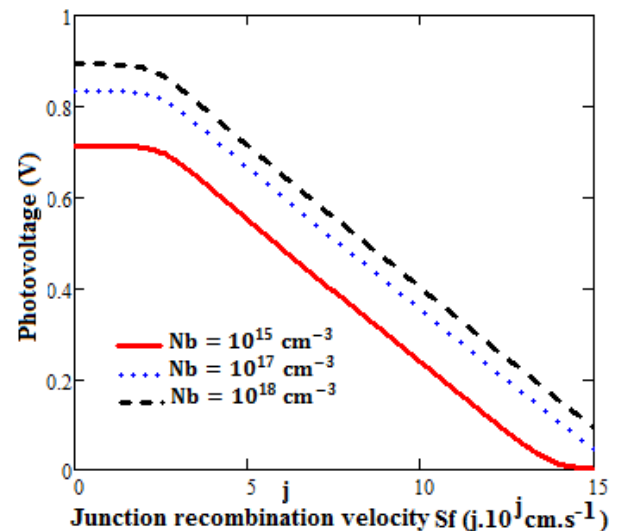


Figure 9: photovoltage versus junction recombination velocity for different doping rate $z = 0,0002 \text{ cm}$; $D = 35 \text{ cm}^2. \text{s}^{-1}$; $B = 10^{-3} \text{ T}$; $H = 0,03 \text{ cm}$

We observe an increase of the photovoltage with the doping rate because of the decrease of diffusion coefficient. So the space charge region width is inversely proportional to doping rate: when the doping of the base increases, the space charge zone width decreases, we shall thus have fewer carriers collected by the junction[20].

3.4 Characteristic I-V

Profile of characteristic I-V for various magnetic field B values is given to the following figure:

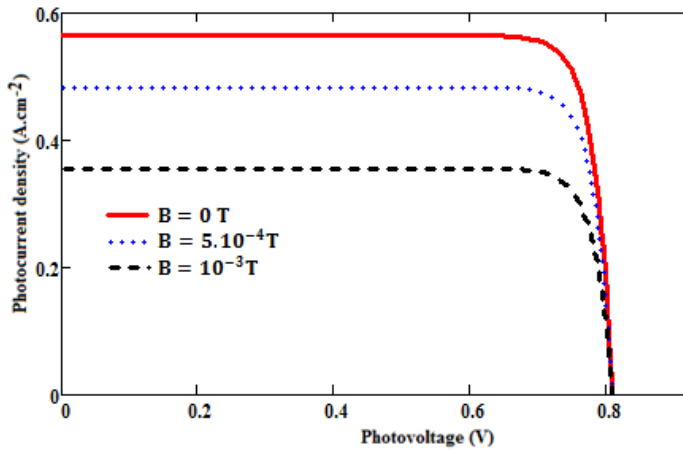


Figure 10: Characteristic I-V for various magnetic field values

$z = 0,0002 \text{ cm}$; $D = 35 \text{ cm}^2, \text{ s}^{-1}$; $N_b = 10^{17} \text{ cm}^{-3}$;
 $H = 0,03 \text{ cm}$

Near short-circuit, photovoltage is low, the current is there almost constant and corresponds at short-circuit current. When the photovoltage aims towards open circuit photovoltage ,photocurrent decreases to nullify. The short-circuit photocurrent and open circuit photovoltage decreases with magnetic field.

We present on the following figure profile of characteristic I-V for various doping rate values:

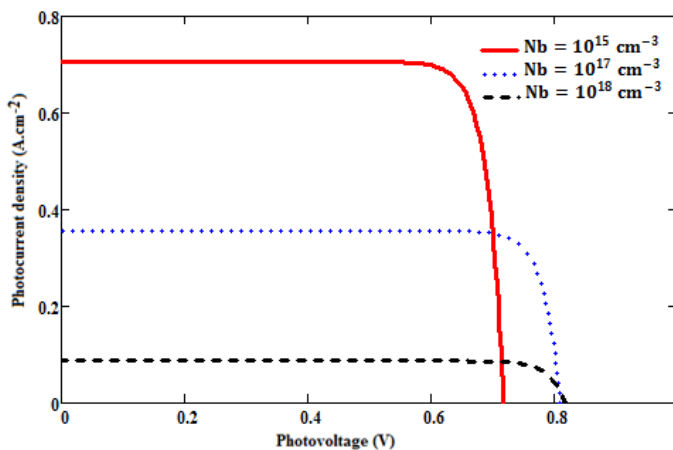


Figure 11: Characteristic I-V for various doping rate values

$z = 0,0002 \text{ cm}$; $D = 35 \text{ cm}^2, \text{ s}^{-1}$; $B = 10^{-3} \text{ T}$;
 $H = 0,03 \text{ cm}$

The short-circuit photocurrent decreases with doping rate of the base and the open circuit photovoltage increases with doping rate.

3.5 Series and shunt resistances study

Series resistance

For determining the series resistance R_s , we propose the equivalent electrical model of the solar cell in open circuit (low values of S_f) where the solar cell operates as photovoltage generator associated to series resistance and the external load (R_L) [21].

The equivalent electrical model of the solar cell near open circuit is represented below:

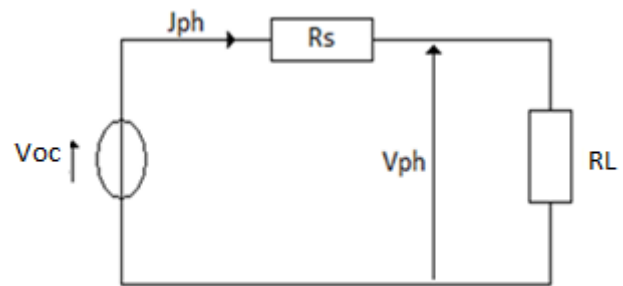


Figure 12: Equivalent electrical circuit of the solar Cell near open circuit

By applying the law of meshes to the circuit of figure 12, we find the expression of series resistance:

$$R_s = \frac{V_{phoc} - V_{ph}(S_f)}{J_{ph}(S_f)} \text{ (Eq - 13)}$$

R_s and R_L are respectively series resistance and external load.

a) Magnetic field effect on series resistance

The profile of series resistance versus junction recombination velocity for various magnetic field values is given on figure 13.

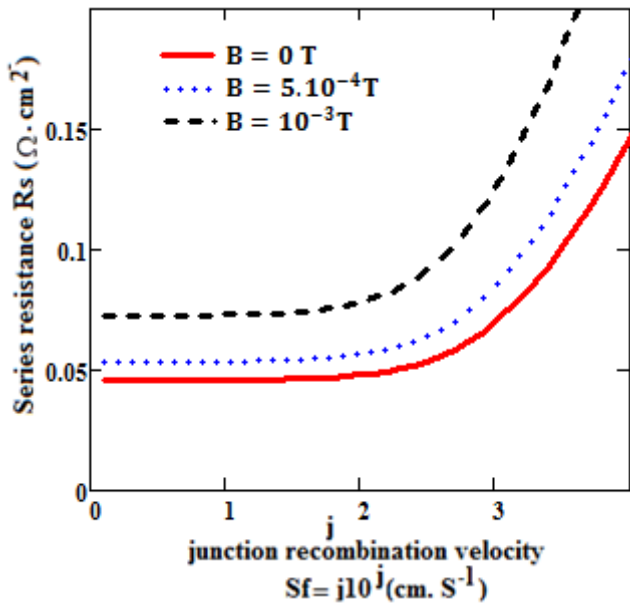


Figure 13:Series resistance versus junction recombination velocity for various magnetic field values
 $z = 0,0002 \text{ cm}$; $D = 35 \text{ cm}^2 \cdot \text{s}^{-1}$; $N_b = 10^{17} \text{ cm}^{-3}$;
 $H = 0,03 \text{ cm}$

b) Doping rate effect on series resistance

On figure 14, we give the profile of series resistance versus junction recombination velocity for various doping rate.

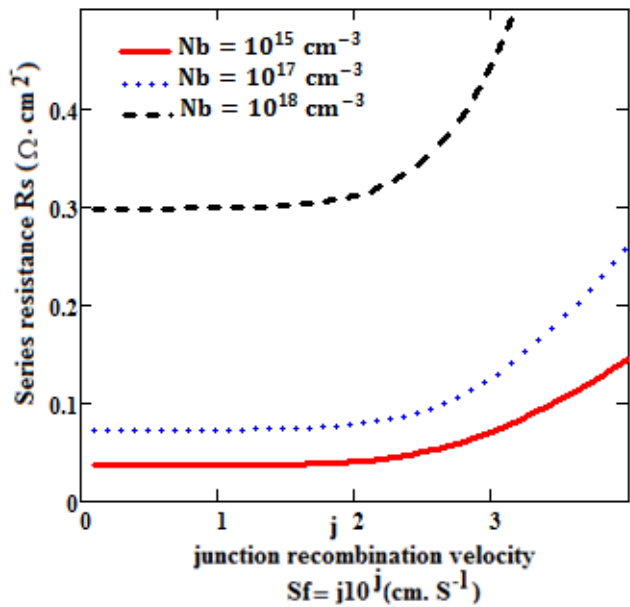


Figure 14:Series resistance versus junction recombination velocity for various doping rate values
 $z = 0,0002 \text{ cm}$; $D = 35 \text{ cm}^2 \cdot \text{s}^{-1}$; $B = 10^{-3} \text{ T}$;
 $H = 0,03 \text{ cm}$

From figures 13 and 14, series resistance is constant for low Sf value(open circuit condition), and varies significantly with the doping rate and less sensitive with the magnetic field.

Shunt resistance

For determine the shunt resistance Rsh, the equivalent electrical model of the solar cell in short circuit (high Sf values ($4 \cdot 10^4 \text{ cm} \cdot \text{s}^{-1} < Sf < 6 \cdot 10^6 \text{ cm} \cdot \text{s}^{-1}$) is proposed. In short circuit situation the solar cell is presented as current generator in parallel with the shunt resistance and with the external charge R_L [22]. The illustrative model of this device is given to the figure 15:

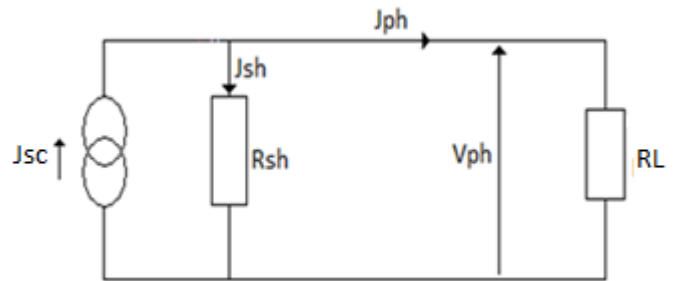


Figure 15: Equivalent electrical model of the solar cell near short circuit

By applying the nodes law to the circuit 15, we find the expression of the shunt resistance is obtained as

$$R_{Sh} = \frac{V_{ph}(Sf)}{J_{phsc} - J_{ph}(Sf)} \quad (\text{Eq} - 14)$$

Where J_{phsc} is the short-circuit photocurrent; its expression is determined from the following relation:

$$J_{phsc} = \lim_{Sf \rightarrow \infty} J_{ph} \quad (\text{Eq} - 15)$$

R_{Sh} and R_L are respectively the shunt resistance and the external load.

a) Magnetic field effect on shunt resistance

We represent at figure 16 the shunt resistance versus junction recombination velocity for various magnetic field B values.

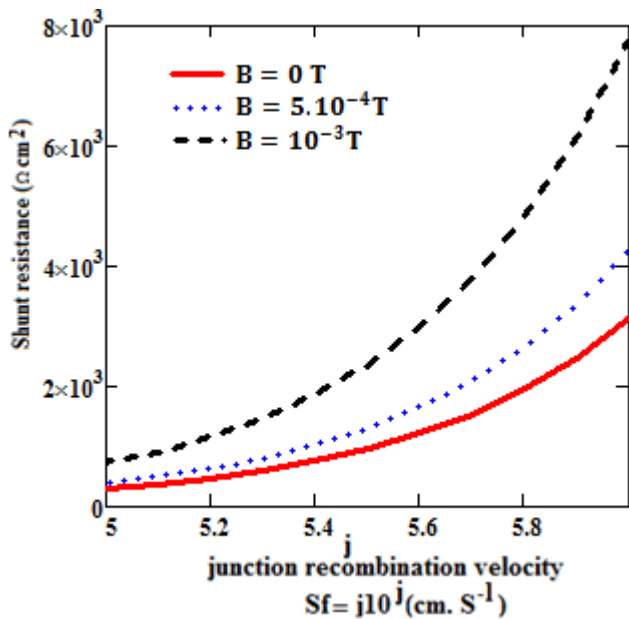


Figure 16: Shunt resistance versus junction recombination velocity for various magnetic field values
 $z = 0,0002 \text{ cm}$; $D = 35 \text{ cm}^2, \text{ s}^{-1}$; $Nb = 10^{17} \text{ cm}^{-3}$;
 $H = 0,03 \text{ cm}$

b) Doping rate effect on shunt resistance

Figure 17 is the plot of shunt resistance versus junction recombination velocity for different Nb values.

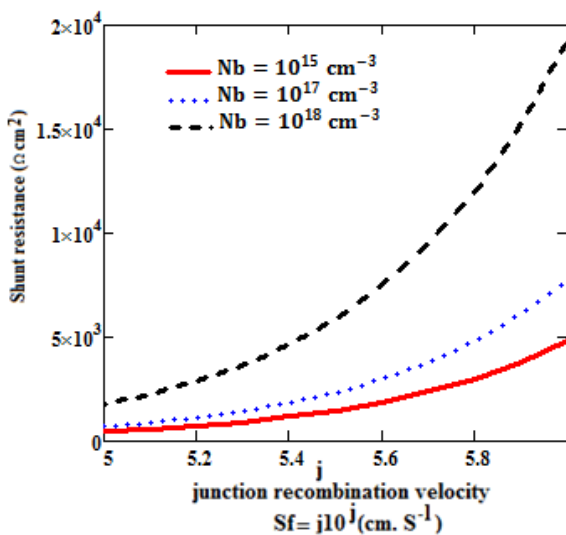


Figure 17: Shunt resistance versus junction recombination velocity for various doping rate values
 $z = 0,0002 \text{ cm}$; $D = 35 \text{ cm}^2, \text{ s}^{-1}$; $B = 10^{-3} \text{ T}$;
 $H = 0,03 \text{ cm}$

Figures 16 and 17, show an exponential increase of Rsh with junction recombination velocity. Increase is important in the case of varying doping rate compare to the applied magnetic field one.

3.6 Capacity study:

The capacity is obtained from the following expression:

$$C = \frac{\partial Q}{\partial V_{ph}} \text{ (Eq - 16)}$$

Calculation leads to:

$$C = C_0 + \frac{q \cdot \delta(0)}{V_T} \text{ (Eq - 17)}$$

With

$$C_0 = \frac{q \cdot ni^2}{Nb} \text{ (Eq - 18)}$$

C_0 is the intrinsic capacity of the solar cell under dark (transition capacity due to fixed charges constituting the Space Charge Region).

a) Magnetic field effect on capacity :

Figure 18 shows capacity variation versus junction surface recombination velocity Sf for various magnetic field values:

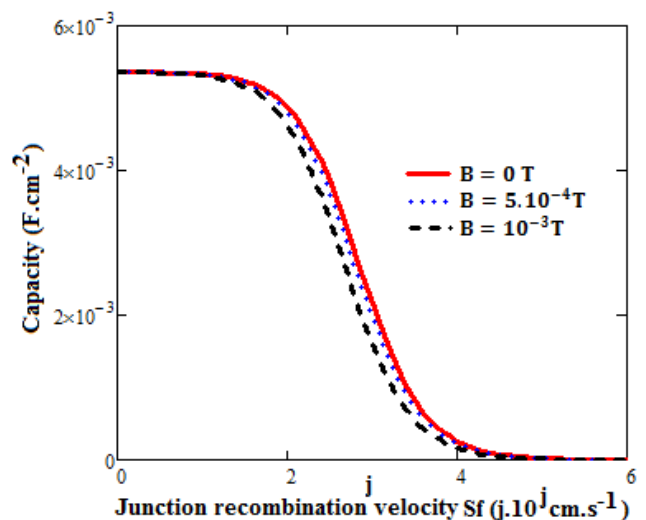


Figure 18 :Capacity versus junction recombination velocity for various magnetic field values

$N_b = 10^{17} \text{ cm}^{-3}$; $D = 35 \text{ cm}^2 \cdot \text{s}^{-1}$; $z = 0,0002 \text{ cm}$;
 $H = 0,03 \text{ cm}$

The capacity is maximal and almost constant for the low junction recombination velocity values ($S_f < 2 \cdot 10^2 \text{ cm/s}$) corresponding to open circuit situation. This is due to the significant number of carriers stored at junction which reduce the space charge region (SCR) and we obtain an increase of the capacity. For the high junction recombination velocity ($S_f > 4 \cdot 10^4 \text{ cm/s}$) corresponding to short-circuit situation, the capacity decreases strongly. This is due to the significant number of carriers which cross the junction and we note an extension of the SCR and thus the decrease of the capacity. The capacity decreases with magnetic field but the low magnetic field values ($B < 10^{-4} \text{ T}$) have not a remarkable effect on the capacity. More the field is intense, more the charge carriers density decreases at junction.

Figure 19 below presents the logarithm of the capacity versus photovoltage for various magnetic field values:

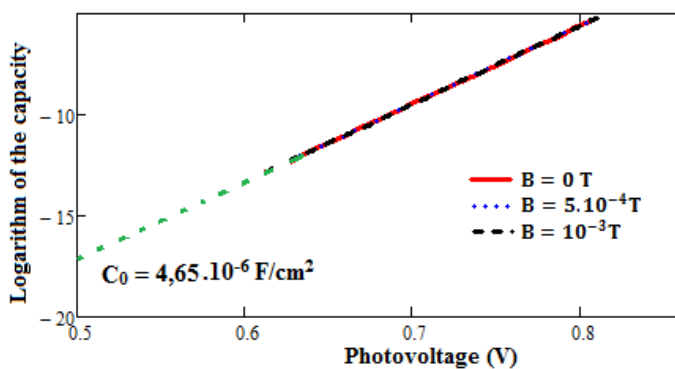


Figure 19: Logarithm of the capacity versus photovoltage for various magnetic field values

$N_b = 10^{17} \text{ cm}^{-3}$; $D = 35 \text{ cm}^2 \cdot \text{s}^{-1}$; $z = 0,0002 \text{ cm}$;
 $H = 0,03 \text{ cm}$

The logarithm of the capacity according to photovoltage is a linear straight of slope $1 / VT$. The ordinate

originally corresponds to $\ln(C_0)$ value. We notice that various curves present the same slope. We can say that the capacity under dark C_0 does not depend on the applied magnetic field value. An extrapolation of these curves on ordinate axis allows us to determine the transition capacity C_0 of the solar cell [23]. The C_0 value obtained after extrapolation on ordinate axis is $C_0 = 4,65 \cdot 10^{-6} \text{ F/cm}^2$.

b) Doping rate effect on capacity:

Profile of the capacity versus junction recombination velocity or different doping rate values N_b is represented on the following figure:

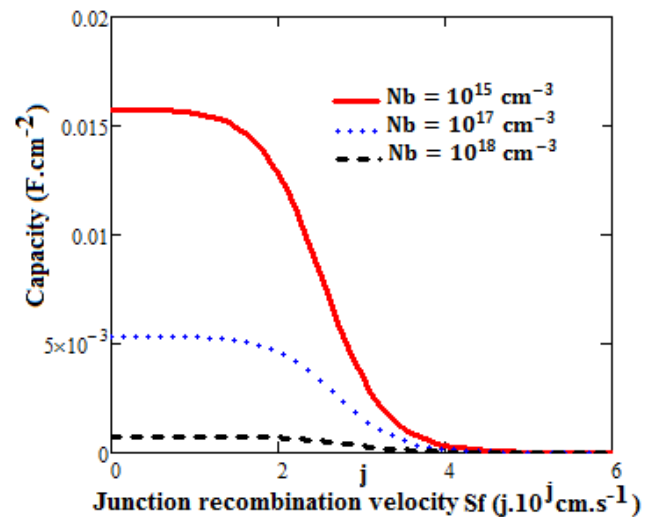


Figure 20 :Profile of the capacity versus junction recombination velocity for different doping rate values N_b

$B = 10^{-3} \text{ T}$; $D = 35 \text{ cm}^2 \cdot \text{s}^{-1}$; $z = 0,0002 \text{ cm}$; $H = 0,03 \text{ cm}$

We note a decrease of the capacity with the doping rate of the base. The recombination of carriers increase with the doping of the base, what entails a decrease of the minority carriers stored and thus a decrease of the capacity.

Figure 21 below presents the logarithm of the capacity versus photovoltage for various doping rate values:

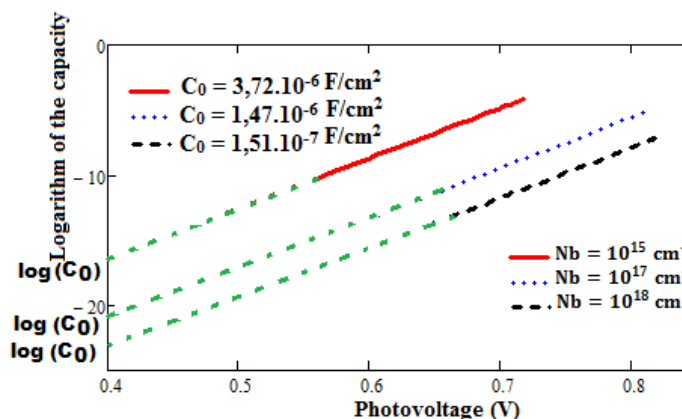


Figure 21: Logarithm of the capacity versus photovoltage for different doping rate values

$$B = 10^{-3} \text{ T}; \quad D = 35 \text{ cm}^2 \cdot \text{s}^{-1}; \quad z = 0,0002 \text{ cm};$$

$$H = 0,03 \text{ cm}$$

These curves also present a linear evolution. We can say that the capacity without illumination C_0 depends on the doping rate value because an extrapolation of every curve on ordinate axis gives us a particular intrinsic capacity value.

Conclusion

In our study we were interested at the effects of the doping rate and of the magnetic field on a parallel vertical junction silicon solar cell under multispectral illumination in static regime. We showed that the photocurrent density decreases with magnetic field and the doping rate. The photovoltage decreases when the magnetic field increases, but then it increases with the doping rate. Series and shunt resistances are deduced from electrical model and are influenced by either the doping rate or the applied magnetic field. The capacity decreases with the magnetic field and the doping rate of the base.

We also obtained as result that the intrinsic capacity depends on the doping rate; it doesn't depend on magnetic field.

Referencies

- [1] B. Equer, "Energie solaires photovoltaïque", volume 1, Collection Ellipses, 1993.
- [2] R.M. Lago-Aurrekoetxea, C. del Cañizo, I. Pou, and A. Luque "Fabrication process for thin silicon solar cells", Proc. 17th European PVSEC, (Munich, 2001) 1519-1522.
- [3] N. Bordin, L. Kreinin, N. Eisenberg, "Determination of recombination parameters of bifacial silicon cells with a two layer step-like effect distribution in the base region", Proc. 17th European PVSEC, (Munich, 2001) 1495-1498.
- [4] Daniel. L. Meier, Jeong-Mo Hwang, Robert B. Campbell. IEEE Transactions on Electron Devices, vol. ED-35, No.1, 1988, pp.70 – 78.
- [5] A. Hübner, A.G. Aberle, and R. Hezel 20% Efficient Bifacial Silicon Solar Cells, 14th European PVSEC, (Munich, 2001) pp 1796 – 1798.
- [6] Jose Furlan and Slavko Amon, "Approximation of the carrier generation rate in illuminated silicon", Solid State Electr, Vol.28, No.12, pp.1241-1243 (1985)
- [7] Harold J. Hovel "semiconductors and semimetals" volume 11 Solar Cells ACADEMIC PRESS New York San Francisco London 1975
- [8] M. I. Ngom, B. Zouma, M. Zougrana, M. Thiame, Z. N. Bako, A. G. Camara, G. Sissoko "Theoretical study of a parallel vertical multi-junction silicon cell under multispectral illumination: influence of external magnetic field on the electrical parameters" International Journal of Advanced Technology & Engineering Research (IJATER); ISSN No:2250-3536 Volume 2, Issue 6, Nov. 2012 pp 101-106.
- [9] S. N. Mohammad, An alternative method for the performance analysis of silicon solar cells, J. Appl. Phys. Vol 61. N^o 2 767-772 1987
- [10] R.M. Lago-Aurrekoetxea, C. del Can, Izo, I. Pou, and A. Luque, "Fabrication Process for thin silicon solar cells", Proc. 17th European PVSEC. (Munich, 2001) 1519-1522
- [11] S. MADOUGOU, F. MADE, M. S. BOUKARY, AND G. SISSOKO I-V Characteristics for Bifacial Silicon Solar Cell studied under a Magnetic field.

Advanced Materials Research Vols. 18-19 (2007) pp. 303-312, online at <http://www.scientific.net> © (2007) Trans Tech Publications, Switzerland - ISSN: 1022-6680 and ISBN: 0-87849-450-2d

[12] **Th. Flohr and R. Helbig**, “Determination of minority-carrier lifetime and surface recombination velocity by Optical-Beam-Induced-Current measurements at different light wavelengths”, J. Appl. Phys. Vol.66 (7), (1989) pp 3060 – 3065.

[13] **A. Dieng, A. Diao, A.S. Maiga, A. Dioum, I. Ly, G. Sissoko**, “A Bifacial Silicon Solar Cell Parameters Determination by Impedance Spectroscopy”, Proceedings of the 22nd European Photovoltaic Solar Energy Conference and Exhibition (2007), pp.436-440.

[14] **D. Mathiot** “Dopage et Diffusion dans le Silicium” Institut d’Électronique du Solide et des Systèmes, InESS, UMR 7163, Laboratoire Commun CNRS – ULP

[15] **Th. Pernau, P. Fath. E. Bucher** Photovoltaics specialists conference, Conference Record of the Twenty-Ninth IEEE, pp 442-445, (2002)

[16] **Sissoko G., C. Museruka, A. Corréa, I. Gaye and A. L. Ndiaye**, 1996. Light spectral effect on recombination parameters of silicon solar cell. Renewable Energy. 3: 1487-1490.

[17] **G. Sissoko, E. Nanema, Y. L. B. Bocande, A. L. Ndiaye, M. Adj** World Renewable Energy Congress (WREC) 1996, part III, pp.1594-1597.

[18] **H.L.Diallo, A. Wereme, A. S. Maïga and G. Sissoko**, 2008. New approach of both junction and back surface recombination velocities in a 3D modelling study of a polycrystalline silicon solar cell. Eur. Phys. J. Appl. Phys., 42: 203–11

[19] **M. M. Dione, S. Mbodji, M. L. Samb, M. Dieng, M. Thiame, S. Ndoye, F. I. Barro, G. Sissoko**, Vertical junction under constant multispectral light: determination of recombination parameters. Proceedings of the 24th European photovoltaic solar energy conference and exhibition, Hamburg, Germany (sept 2009), 465 – 468.

[20] **S. MBODJI, B. MBOW, F. I. BARRO and G. SISSOKO**

A 3D model for thickness and diffusion capacitance of emitter-base junction determination in a bifacial polycrystalline solar cell under real operating condition

Turkish Journal of Physics, 35 (2011) , 281 – 291. <http://journals.tubitak.gov.tr/physics/index.php>

[21] **K. Kotsovos, K. Misiakos**, 16th European Photovoltaic Solar Energy Conference, 1-5 May 2000, Glasgow, UK

[22] **E.SOW, S. MBODJI, B. ZOUMA, M. ZOUNGRANA, I. ZERBO, A. SERE and G. SISSOKO**.

“Determination in 3D modeling study of the width emitter extension region of the solar cell operating in open circuit condition by the Gauss’s Law.”

International Journal of Science, Environment and Technology (IJSET), Volume 1, N°4,

pp. 230 – 246, 2012; <http://www.ijset.net>.

[23] **G. Sissoko, B. Dieng, A. Correa, M. Adj and D. Azilinin**, “Silicon Solar Cell Space Charge Region Width Determination by Modelling Study”, Proceeding of the World Renewable Energy Conference and Exhibition, (1998), pp.1852 – 1855.